Title

Functional Relevance of Interleukin-1 Receptor Inter-domain Flexibility for Cytokine Binding and Signaling

Journal

Structure, 27(8)

ISSN

1359-0278

Authors

Ge, Jiwan

Remesh, Soumya G

Hammel, Michal

et al.

Publication Date

2019-08-01

DOI

10.1016/j.str.2019.05.011

Peer reviewed

HHS Public Access

Author manuscript

Structure. Author manuscript; available in PMC 2020 August 06.

Published in final edited form as:

Structure. 2019 August 06; 27(8): 1296–1307.e5. doi:10.1016/j.str.2019.05.011.

Functional Relevance of IL-1 Receptor Inter-domain Flexibility for Cytokine Binding and Signaling

Jiwan Ge[1,6], **Soumya G. Remesh**[2,6], **Michal Hammel**[2], **Si Pan**[1], **Andrew D. Mahan**[3], **Shuying Wang**[4,5,*], **Xinquan Wang**[1,7,*]

[1]Ministry of Education Key Laboratory of Protein Science, Beijing Advanced Innovation Center for Structural Biology, Beijing Frontier Research Center for Biological Structure, Collaborative Innovation Center for Biotherapy, School of Life Sciences, Tsinghua University, Beijing 100084, China

[2]Molecular Biophysics and Integrated Bioimaging, Lawrence Berkeley National Laboratory, Berkeley, California 94720, USA

[3]Jassen Bio Therapeutics, Janssen R&D, LLC, Spring House, PA 19477, USA

[4]Department of Microbiology and Immunology, National Cheng Kung University Medical College, Tainan 701, Taiwan

[5]Center of Infectious Disease and Signaling Research, National Cheng Kung University, Tainan 701, Taiwan

[6]These authors contributed equally

[7]Lead Contact

SUMMARY

The interleukin 1 (IL-1) receptor family, whose members contain three Ig-like domains (D1-D3) in the extracellular region, is responsible for transmitting pleiotropic signals of IL-1 cytokines. The inter-domain flexibility of IL-1 receptors and its functional roles have not been fully elucidated. In this study, we used small-angle X-ray scattering (SAXS) to show that ligand-binding primary receptors and co-receptors in the family all have inherent inter-domain flexibility due to the D2/D3 linker. Variants of the IL-1RAcP and IL-18Rβ co-receptors with mutated D2/D3 linkers cannot form a cytokine-receptor complex and mediate signaling. Our analysis further revealed that these mutated co-receptors exhibited a changed conformational ensemble, suggesting that loss of

*Correspondence: xinquanwang@mail.tsinghua.edu.cn(XQ.W.), sswang23@mail.ncku.edu.tw(SY.W.).

AUTHOR CONTRIBUTIONS

Protein expression was performed by JW. G. and S. P.. Surface plasmon resonance analysis, IL-1RAcP knockout cell line construction, dual-luciferase reporter assay were performed by JW. G.. SAXS data collection was performed by M. H. and SY. W.. Solution structure modelling was performed by S. G. R., M. H. and JW. G.. Mass spectroscopy was performed by A. D. M.. SY. W., XQ. W., JW. G. prepared the manuscript. M. H. and S. G. R. revised the manuscript. XQ. W. and SY. W. were responsible for project direction. All authors reviewed the results and approved the final version of the manuscript.

DECLARATION OF INTERESTS

The authors declare no competing interests.

function is due to the alteration of receptor dynamics. Taken together, our results demonstrate that the D2/D3 linker is a critical functional determinant of IL-1 receptor and underscore the important roles of the inter-domain flexibility in cytokine/receptor binding and signaling.

Graphical Abstract

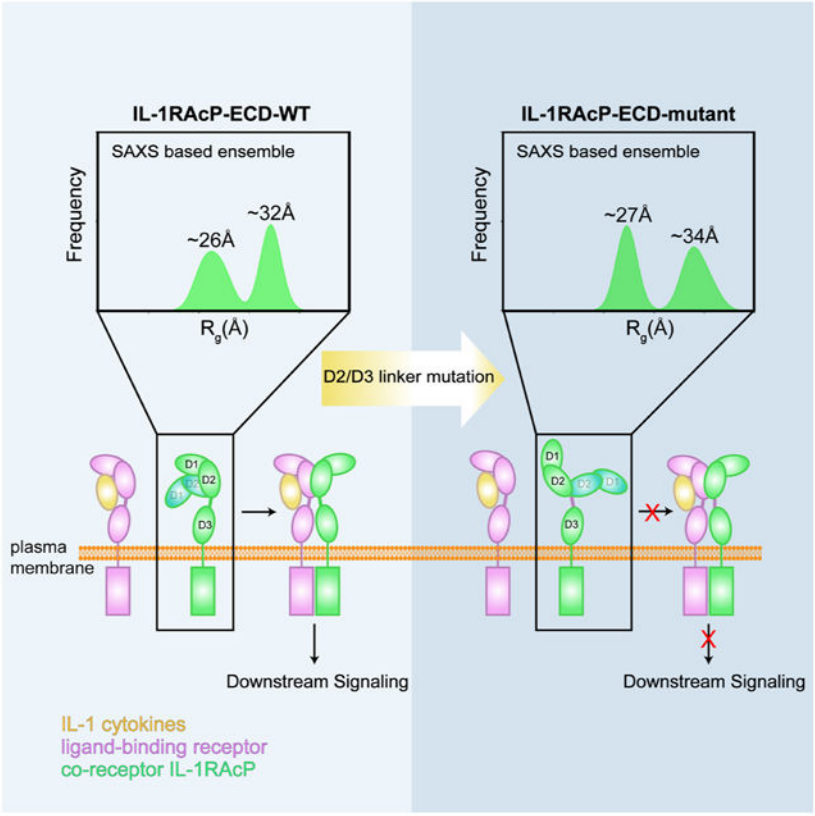

eTOC Blurb

The IL-1 receptors are responsible for transmitting signaling in immune responses. Jiwan et al. investigated the effect of a common D2/D3 linker within IL-1 receptors and revealed the functional role of inherent inter-domain flexibility in ligand recognition and signal transduction.

Keywords

Inter-domain flexibility; IL-1 receptor family; small-angle X-ray scattering (SAXS); signal transduction; dual-luciferase reporter assay; minimal ensemble search (MES)

INTRODUCTION

Ligand-receptor interactions are widely viewed as dynamic and intricate processes rather than a rigid lock-and-key binding event (Gunasekaran et al., 2004, Koshland, 1958), especially in the case of multi-domain receptors with inter-domain linkers. These linkers usually result in significant inter-domain flexibility of receptors which play important roles

in ligand recognition and receptor activation. Therefore, considerable attention has been focused on the properties and roles of the inter-domain linkers in protein interactions (Bruning et al., 2010, Gokhale and Khosla, 2000, Wriggers et al., 2005). Recently, our knowledge on ligand recognition and receptor activation in the IL-1 superfamily of cytokines and receptors has been greatly enriched by the determined ligand-receptor ternary complex structures at atomic resolution(Wang et al., 2010, Thomas et al., 2012, Tsutsumi et al., 2014, Gunther et al., 2017). However, the important roles of flexibility, especially the inter-domain flexibility of IL-1 receptors comprising multiple extracellular domains, cannot be fully revealed by these static complex structures. Therefore, investigating protein flexibility in IL-1 receptors by combining classical structural determination with other biochemical, biophysical and biological assays is very important for a full understanding of ligand-receptor association.

The IL-1 superfamily of cytokines and receptors are pivotal players in the activation and regulation of innate and adaptive immune responses and in many immunopathological disorders (Dinarello, 2002, Sims and Smith, (2010). There are eleven members in the IL-1 cytokine family, including seven agonists (IL-1α, IL-1β, IL-18, IL-33, IL-36α, IL-36β and IL-36γ), three receptor antagonists (IL-1Ra, IL-36Ra and IL-38), and one anti-inflammatory cytokine (IL-37) (Garlanda et al., 2013a, Palomo et al., 2015). The extended IL-1 receptor family comprises of the primary receptors IL-1RI, IL-1RII, ST2, IL-1Rrp2 and IL-18Rα which binds to ligands with high affinities, the co-receptors IL-1RAcP and IL-18Rβ which do not directly bind to ligands but are essential for signaling (Cullinan et al., 1998), the inhibitory receptor SIGIRR (Garlanda et al., 2013a, Polentarutti et al., 2003) and the two orphan receptors TIGIRR-1 and TIGIRR-2 (Born et al., 2000, Garlanda et al., 2013b). The IL-1 receptors are single-pass transmembrane proteins and all family members possess three immunoglobulin (Ig)-like domains (D1-D3) in the extracellular region, with the exception of SIGIRR, which has only one Ig-like domain. Members of IL-1 receptors except IL-1RII (McMahan et al., 1991) contain an intracellular Toll/Interleukin-1 receptor (TIR) domain for signal transduction.

The IL-1-mediated signaling cascade is initiated by agonist cytokines binding to the extracellular domain (ECD) of their primary ligand-recognition receptor and then recruiting a co-receptor to form a ternary signaling complex, which juxtaposes the intracellular TIR domains of receptors and subsequently triggers the activation of the NF-κB and MAPK pathways (Adachi et al., 1998, Bowie and O'Neill, 2000, O'Neill, 2008a, O'Neill). The primary receptors IL-1RI and IL-1Rrp2 are promiscuous and capable of binding to different agonists. IL-1RI can bind to IL-1α and IL-1β, while IL-1Rrp2 can bind to IL-36α, IL-36β and IL-36γ (Debets et al., 2001, Towne et al., 2004, Towne et al., (2011). By contrast, ST2 and IL-18Rα specifically recognize IL-33 and IL-18, respectively. The shared co-receptor IL-1RAcP is recruited by preformed binary complexes such as IL-1α/IL-1Rl, IL-1β/IL-1Rl, IL-33/ST2, IL-36α/IL-1 Rrp2, IL-36β/IL-1Rrp2 and IL-36γ/IL-1Rrp2, whereas the IL-18-specific co-receptor IL-18Rβ is recruited only by the IL-18/IL-18Rα complex (Figure S1). Receptor antagonists in the IL-1 family exert their inhibitory effect by competitively binding to the primary receptor and inhibiting the recruitment of the co-receptor. Another negative regulation effect is exerted by decoy and inhibitory receptors such as IL-1RII (Colotta et al., 1993) and SIGIRR (Qin et al., 2005, Wald et al., 2003). IL-1RII, which lacks the

intracellular TIR domain, binds IL-1α or IL-1β with high affinity and then recruits IL-1RAcP into a non-signaling ternary complex. SIGIRR, as a negative regulator, inhibits IL-1 signaling by preventing adaptor proteins from binding to IL-1 receptors and thus blocks NF-κB and MAPK activation (Wald et al., 2003, Qin et al., 2005).

The available crystal structures of ternary complexes, determined by our group and others, include the non-signaling complex IL-1β/IL-1RII-ECD/IL-1RAcP-ECD (Wang et al., 2010) and the signaling complexes IL-1β/IL-1RI-ECD/IL-1RAcP-ECD (Thomas et al., 2012), IL-33/ST2-ECD/IL-1 RAcP-ECD (Gunther et al., 2017) and IL-18/IL-18Rα-ECD/IL-18Rβ-ECD (Tsutsumi et al., 2014, Wei et al., 2014). The extracellular portions of primary receptors with D1-D3 Ig-like domains have a shape that resembles a question mark, with a long D2/D3 linker connecting the D3 domain to the D1D2 module. Two disparate binding sites in the concave surface, site I in the D1D2 module and site II in the D3 domain, participate in cytokine binding. At the binding interface, site I contributes most of the cytokine-receptor interactions and site II wraps around the other side of the bound cytokine. The flexibility of the D2/D3 linker is crucial for orientating the D3 domain to bind the cytokine and to form a stable complex. The binary complex then recruits the co-receptor through extensive D2-D2 and D3-D3 interactions between the primary receptor and the co-receptor. Although these structural results helped reveal the activation mechanism, all current structures of IL-1 receptors were determined in ligand-bound state, while the ligand-receptor binding and assembly process is not yet well understood. Due to the critical role of the D3 domain in ligand binding and receptor assembly, we hypothesized that the naturally occurring D2/D3 linker sequence within each receptor plays a significant role in its biological function.

Small-angle X-ray scattering (SAXS) is a powerful tool to experimentally probe protein flexibility and to elucidate the functionally relevant conformations to provide insights into the relationship between flexibility and function (Hammel, 2012, Pelikan et al., 2009, Remesh et al., 2018, Puz et al., 2017, Tossavainen et al., 2018, Bernado et al., 2007, Bernado and Svergun, 2012). We previously determined the solution conformations of the ECD of the IL-33-specific primary receptor ST2 and the co-receptor IL-1RAcP, and proposed a two-step binding model (Liu et al., 2013). Here we extended the SAXS study to other IL-1 primary receptors, including IL-1RI-ECD, IL-1RII-ECD, IL-18Rα-ECD and the other co-receptor IL-18Rβ-ECD. Furthermore, we investigated the functional role of the D2/D3 natural linker sequence of the shared co-receptor IL-1RAcP and IL-18Rβ in cytokine-receptor complex formation and signaling, using a combination of linker mutagenesis, SAXS, surface plasmon resonance (SPR) and cell-based luciferase reporter assay. Our results revealed the commonality of inherent inter-domain flexibility exhibited by IL-1 receptors and demonstrated that the D2/D3 natural linker sequences are crucial determinants of the flexibility-dependent function of IL-1RAcP and IL-18Rβ in complex assembly and signal transduction.

RESULTS

The Inter-domain Flexibility and Conformations of IL-1 Receptors in Solution

Our previous work revealed that the IL-33-specific receptor ST2, having a long and extended D2/D3 linker between the D1D2 module and D3 domain, possesses high inter-domain flexibility, whereas its co-receptor IL-1RAcP is less flexible (Liu et al., 2013). Here we performed SAXS studies to experimentally assess the inter-domain flexibility of other IL-1 receptors and explored the relevant conformations in solution.

The primary receptors IL-1RI, IL-1RII and IL-1Rrp2 also utilize the co-receptor IL-1 RAcP for signaling. Similar to the ST2-ECD and IL-1RAcP-ECD we previously studied, recombinant IL-1RI-ECD and IL-1 RII-ECD proteins, displayed monodisperse elution profiles in size-exclusion chromatography (Figure S2A). SEC-SAXS (size-exclusion chromatography in-line with SAXS data collection) was carried out for IL-1RI-ECD and IL-1RII-ECD to ensure that the scattering curves were collected using the aggregation-free state of the samples. Guinier plots of the SAXS data showed a linear dependence of log(I(q)) with q^2 and unbiased residuals, confirming that the samples were monodisperse (Table S1 and Figure S3A). The molecular weight of the receptors determined from the experimental SAXS profiles using the volume of correlation Vc (Rambo and Tainer, 2013) were also consistent with the theoretical mass (Table S1).

The primary receptors IL-1RI-ECD, IL-1RII-ECD and ST2-ECD and their co-receptor IL-1RAcP-ECD showed differences in the normalized Kratky plots, indicating variations in their overall architecture as well as peaks-shifts useful to evaluate the extent of inter-domain flexibility (Figure 1 A). The normalized Kratky plot shown in Figure 1A illustrates that IL-1RII-ECD (red) is the least flexible while IL-1RI-ECD (black) is the most flexible. The pair-distribution function P(r) further supports distinct conformational sampling of individual receptors in solution (Figure 1B). While IL-1RII-ECD (red) appears to have a more bell-shaped P(r) function with a single peak, IL-1RI-ECD, ST2-ECD and IL-1RAcP-ECD each has distinct P(r) function (Figure 1B).

To further confirm the inter-domain flexibility and to elucidate the relevant states of IL-1 receptors in solution, we performed conformational sampling based on molecular dynamics simulation using BILBOMD (Pelikan et al., 2009) and minimal ensemble search implemented in MultiFoXS (Schneidman-Duhovny and Hammel, 2018, Schneidman-Duhovny et al., 2016) to model the population of conformations adopted by IL-1RI-ECD, IL-1RII-ECD, ST2-ECD and IL-1RAcP-ECD. To map the glycosylation sites and the glycan forms of the IL-1 receptors expressed in insect cells in this study, we performed a comprehensive mass spectrometric analysis (Table S2) and constructed full-atom models of glycosylated IL-1RI-ECD, IL-1RII-ECD, ST2-ECD and IL-1RAcP-ECD. The scoring function and fit parameters in SAXS are sensitive to the missing atoms of an input atomic model (Brooks et al., 2009), therefore a full-atom model was built before performing the simulation.

After defining the linker between the D1D2 module and the D3 domains (D2/D3 linker) as flexible, ~10,000 conformations were sampled. The resulting SAXS-based modeling showed

that the best-fitting models of the glycosylated IL-1 receptors were in significantly better agreement with the experimental SAXS data than the initial crystal structures (Figure 1C and Table S3). In addition, the fitting of experimental SAXS data was further improved by selecting a two-state ensemble. Here to compare conformational variability between IL-1 receptors we focused only on the two-state ensemble rather than the higher-state ensembles. Two-state ensemble analysis characterized here do not represent static state, but rather show the differential conformational space adopted by the D3 domain. The weighted R_g distribution for the two-state ensemble showed that the range of accessible conformations was clustered around the open and closed conformer (Figure 1D), whereas the height of the peak in the R_g distribution reflected the dominance of the conformers in the solution. The individual conformers are not as significant as the evidence that an ensemble represents the solution state better, which hints at the intrinsic D2/D3 linker flexibility. For IL-1RII, the weighted R_g distribution revealed that the two-state ensemble of IL-1RII-ECD in solution was predominantly in the closed state (R_g~24A) and was in agreement with the comparison of the normalized Kratky plot which indicated a more compact structure (Figure 1A).

Our previous work on ST2-ECD and IL-1RAcP-ECD did not include glycans for modeling and fitting. We therefore revisited our published data to investigate the degree of inter-domain flexibility of ST2 and IL-1RAcP. A shift of the peak in the normalized Kratky plot confirmed that ST2-ECD exhibits more flexibility than IL-1RAcP-ECD (Figure 1A). With the new glycosylated models, we show equal contribution of closed and open conformers for ST2-ECD in R_g distribution, which hints at the intrinsic D2/D3 linker flexibility. The less flexible IL-1RAcP-ECD exists largely in an open state (R_g~32Å), as evidenced by the higher weight for this state in the R_g distribution (Figures 1C and 1D).

Our analyses showed that the two more flexible receptors IL-1RI-ECD and ST2-ECD likely screen a range of conformers between the two states presented here (Figures 1C and 1D). Conversely, IL-1RII-ECD and IL-1RAcP-ECD mostly exist as one of the two extreme conformers, closed or open in solution. Taken together, our SAXS experiments demonstrate that IL-1 receptors adopt a range of closed and extended conformations that co-exist in solution.

Impaired Function of IL-1RAcP Mutants with Swapped D2/D3 Linker from Primary Receptors

SAXS analysis showed that the flexible D2/D3 linker generates the dynamic ensemble of IL-1 receptors. The alignment of all D2/D3 linkers of IL-1 receptors did not reveal an amino acid sequence or pattern that may be responsible for the inherent inter-domain flexibility (Figure S2B). To explore the role of linker sequence in the biological function of IL-1 receptors, we designed a series of linker mutations by systematically swapping the D2/D3 linker between IL-1RAcP and primary receptors. However, the modified IL-1RI-ECD, IL-1RII-ECD, ST2-ECD and IL-1Rrp2-ECD with the swapped D2/D3 linker stemming from IL-1RAcP (^{234}VGSPKNAVP^{242}) could not be expressed well in insect cells. IL-1RAcP-ECD mutants with the linker from IL-1Rl (^{218}LEENKPTR^{225}), IL-1Rll (^{229}KKKKEETI^{236}) or ST2 (^{203}KDEQGFSLF^{211}) (Figure S2B) were successfully expressed and purified, and

were marked as IL-1RAcP-ECD-RI, IL-1RAcP-ECD-RII and IL-1RAcP-ECD-ST2, for the following experiments.

We first assessed whether the IL-1RAcP-ECD mutants are capable of forming the ternary complex with the preformed binary complexes IL-1β/IL-1RI-ECD and IL-33/ST2-ECD using SPR (Figure 2A). The dissociation constant was 6 and 31 nM, respectively (Figures 2B and 2C). By contrast, the binding affinities of the IL-1RAcP-ECD mutants IL-1RAcP-ECD-RI, IL-1RAcP-ECD-RII and IL-1RAcP-ECD-ST2 to the IL-1β/IL-1RI-ECD and IL-33/ST2-ECD complexes were all dramatically decreased to an undetectable level (Figures 2B and 2C). Furthermore, we performed circular dichroism (CD) analysis of IL-1RAcP mutants to verify their intact secondary structure (Figure S5A).

To further investigate the effect of the D2/D3 linker replacement on IL-1RAcP function, we examined whether IL-1RAcP-RI, IL-1RAcP-RII and IL-1RAcP-ST2 affect signal transduction by using a dual-luciferase reporter assay for cytokine-triggered and IL-1RAcP-mediated activation of NF-κB in HEK 293T cells. To exclude interference from the endogenously expressed IL-1RAcP (Huang et al., 1997), we generated a HEK 293T cell line with the *IL-1RAcP* gene knockout (293T-IL-1RAcP-KO) using the CRISPR/Cas9 system (Sanjana et al., 2014, Shalem et al., 2014) (Figure S4). The plasmids encoding the wild-type IL-1RAcP and the mutants (IL-1RAcP-RI, IL-1RAcP-RII and IL-1RAcP-ST2) were then reintroduced into the 293T-IL-1RAcP-KO cells. Due to the endogenous expression of IL-1RI, the IL-1β-mediated NF-κB signaling was tested without the co-transfection of the primary receptor IL-1RI. When stimulated with IL-1β, the IL-1RAcP mutants lost the ability to mediate the signal transduction, as evidenced by the decrease of the luciferase signal to the basal level (Figure 3A). For the examination of IL-33- and IL-36γ-mediated NF-κB signaling, the primary receptor ST2 or IL-1Rrp2 was co-transfected into the 293T-IL-1RAcP-KO cells with IL-1RAcP or its mutants. The ability of IL-1RAcP to transduce IL-33 and IL-36γ-mediated NF-κB signaling was also abolished after the replacement of the D2/D3 linker (Figures 3B and 3C). To confirm that the decreased luciferase signal was not due to decreased expression levels of IL-1RAcP mutants, we verified that IL-1RAcP and its mutants were expressed at the same level by western blot analysis (Figures 3A-3C) and we also confirmed its localization in the membrane fraction (Figure S5A).

Perturbation of Inter-domain Dynamics in IL-1RAcP Mutants with Swapped D2/D3 Linker

The impaired function of the described IL-1RAcP mutants with swapped D2/D3 linker may result from the exchange of specific residues involved in forming the ternary signaling complex. Previous structural studies have shown that the recruitment of IL-1RAcP relies on the D2-D2 and D3-D3 interactions between IL-1RAcP and the primary receptor, and only the two residues K238 and N239 located at the IL-1RAcP D2/D3 linker are involved in the binding interface with preformed IL-1β/IL-1RI-ECD and IL-33/ST2-ECD complexes (Figure S6) (Gunther et al., 2017). Using SPR, Eric *et al* recently showed that the IL-1RAcP-ECD-K238A mutant exhibited ~3-fold decreased binding to the IL-1β/IL-1RI-ECD and IL-33/ST2-ECD complexes. The IL-1RAcP-ECD-N239A mutation did not affect the binding to the IL-1β/IL-1RI-ECD complex and modestly decreased the binding to the IL-33/ST2 complex by ~3-fold (Gunther et al., 2017). By contrast, our experiments showed

that IL-1RAcP-ECD mutants with the swapped D2/D3 linker completely lost their binding affinity for the IL-1β/IL-1RI-ECD and IL-33/ST2-ECD complexes.

We also utilized the NF-κB luciferase reporter assay in the 293T-IL-1RAcP-KO cells to assess the effects of K238A and N239A mutations in IL-1RAcP on signal transduction. When the cells were stimulated with IL-1β, the introduction of K238A, N239A or K238A/N239A mutations in the IL-1RAcP had no effect on the luciferase signal (Figure 4A). Similarly, the single mutants K238A and N239A did not affect the luciferase signal induced by IL-33, whereas the double mutant K238A/N239A decreased the signal by approximately 50% (Figure 4B). For the IL-36γ-stimulated signal, there was also no significant change upon introducing the K238A mutation (Figure 4C). The introduction of the N239A or K238A/N239A mutations into IL-1RAcP reduced the luciferase signal by approximately 50% (Figure 4C). We also confirmed that IL-1RAcP and the site-directed mutants were expressed at the same level in the cell membrane (Figure S5C). Therefore, we concluded that the effects of site-directed mutations in the D2/D3 linker were not as dramatic as the replacement of the D2/D3 linker, which completely abolished the ability of IL-1RAcP to transduce the IL-1-mediated NF-κB signaling of agonists including IL-1β, IL-33 and IL-36γ.

After excluding the effects of site-directed mutations, we further performed SAXS studies on IL-1RAcP-ECD-RI, IL-1RAcP-ECD-RII and IL-1RAcP-ECD-ST2. We collected the scattering data as described above and confirmed the monodispersity of the samples (Figures S2C and S3A). The conformational space occupied by the IL-1RAcP-ECD mutants in solution was assessed as described for the wild-type IL-1RAcP-ECD. The two-state ensemble of IL-1RAcP-ECD mutants fit the experimental data better (Figures 5A, 5B and Table S3). The weighted R_g distributions of the two-state ensemble of the IL-1RAcP-ECD mutants were different from that of the wild-type IL-1RAcP-ECD (Figure 5C). Most interestingly, replacing the IL-1RAcP-ECD linker with that of IL-1Rll (^{229}KKKKEETI^{236}) shifted the conformational sampling in favor of the more closed state (R_g~27Å). Replacing the IL-1RAcP-ECD linker with that from IL-1RI (^{218}LEENKPTR^{225}) and ST2 (^{203}KDEQGFSLF^{211}) also shifted the conformational sampling (Figure 5C). The SAXS analysis suggests the replaced linker within IL-1RAcP may perturb the inter-domain conformational dynamics resulting in loss of function.

Impaired Function and Altered Inter-domain Dynamics of IL-18Rβ with Swapped Linker from IL-18Rα

As the other co-receptor in the IL-1 receptor family, IL-18Rβ is not shared like IL-1RAcP and is only recruited by preformed IL-18/IL-18Rα to form a complex and mediate signaling. We first studied the solution structures of IL-18Rα-ECD and IL-18Rβ-ECD by SAXS. The normalized Kratky plot shown in Figure S3B indicated that IL-18Rβ-ECD is more flexible than IL-18Rα-ECD. SAXS-based modeling revealed that the ensemble of two models with flexible D2/D3 linker for IL-18Rα-ECD fitted the experimental SAXS data well (Figure 6A, left). The fitting significantly improved with both the flexible D1/D2 linker and flexible D2/D3 linker for IL-18Rβ-ECD (Figure 6A, middle). We observed that while IL-18Rα-ECD existed as an ensemble of two states with comparable radii of gyration in solution, IL-18Rβ-

ECD had a considerable proportion of conformers with large radii of gyration and maximal dimension.

To further test whether the flexibility-correlated function of the D2/D3 linker also exists in IL-18Rβ, we also generated an IL-18Rβ-ECD mutant with the D2/D3 linker replaced with that of IL-18Rα, which we named IL-18Rβ-ECD-18Rα. The linker-swapped IL-18Rβ-ECD-18Rα was expressed and purified as the wild-type (Figure 2C). The binding ability and signaling function of IL-18Rβ-ECD-18Rα were also examined using the above-mentioned SPR (Figure 6B) and dual-luciferase reporter assay (Figure 6C). As expected, the replacement of its D2/D3 linker abolished the ability of IL-18Rβ-ECD-18Rα to form a complex and mediate NF-κB signaling (Figure 6C). The crystal structure of the IL-18/IL-18Rα-ECD/IL-18Rβ-ECD complex showed that the D2/D3 linker is not explicitly involved in the binding interface (Tsutsumi et al., 2014) (Figure S6). We also performed SAXS studies on IL-18Rβ-ECD-18Rα and showed that the weighted R_g distribution of the two-state ensemble of IL-18Rβ-ECD-18Rα is considerably different from that of the parent receptor (Figure 6A and Table S3). In addition, CD study showed an intact structure (Figure S5B) and subcellular fraction assay (Figure S5D) suggested a localization of membrane fraction. All these experiments indicated that the natural D2/D3 sequence plays an important role in inter-domain conformational dynamics and the replacement of the linker altered this dynamics, leading to the loss of function of IL-18Rβ-ECD-18Rα.

DISCUSSION

The importance of inter-domain flexibility in protein function has been recognized for a long time (Ferofontov et al., 2018, Ruiz et al., 2016, Puz et al., 2017, Matoba et al., 2017). In this work, we revealed a general dynamic nature of IL-1 receptors by SAXS studies, showing that these receptors with three extracellular Ig-like domains have intrinsic inter-domain flexibility mediated by the D2/D3 linker. Furthermore, we demonstrated that the natural D2/D3 linker sequence is the functional determinant of the inter-domain flexibility-dependent function of co-receptors IL-1RAcP and IL-18Rβ by combining linker-replacement mutagenesis, biochemical characterization, functional assay, SAXS analysis and SAXS-based atomistic modeling.

The conformational ensembles of the IL-1 primary receptors exhibited a spectrum of closed and open conformations in solution, which may allow a ligand to search for the immediate complementary conformation of the pre-existing states of a receptor during the binding process. We also showed that the replacement of the D2/D3 linkers of the co-receptors IL-1RAcP and IL-18Rβ with those of their respective primary receptors completely abolished their ability to form ternary signaling complexes and mediate signal transduction. By excluding the effects of direct interaction, change of secondary structure, or discrepancies of expression in the membrane fraction and showing altered inter-domain dynamics of linker-swapped IL-1RAcP mutants, we suggest that swapping the D2/D3 linker in IL-1RAcP may lead to changes of the D3 positional distribution in which the binding-competent state of IL-1RAcP is not readily available to the cytokine/primary receptor complexes, resulting in the functional disruption of IL-1RAcP in binding and signaling.

As a shared co-receptor, IL-1RAcP is promiscuous in binding to different binary complexes of cytokines with primary receptors. The determined cytokine/receptor complex structures have shown extensive D2-D2 and D3-D3 interactions between IL-1RAcP and respective primary receptors in different signaling complexes, which also indicates that the D2/D3 linker dependent flexibility between the D2 and D3 domains should be an important functional determinant. Currently, there are still no solid experimental data to distinguish whether the role of IL-1RAcP D2/D3 linker in the binding and signaling is to promote a conformational selection or to allow an induced-fit model. These two models are two extreme possibilities, and distinguishing between these two extreme possibilities is facile conceptually, while the experimental determination can be very challenging. It should be noted that studies have also shown that conformational selection is usually coupled with induced-fit, and the two models work together to optimize the protein interactions (Nussinov et al., 2014, Galburt and Tomko, 2017). We suggest that at the first step, a preferred pool of IL-1RAcP D3 positional distributions may facilitate a favorable alignment of the requisite D2 and D3 domains for the initial binding of IL-1RAcP to different cytokine/primary receptor complexes. After the binding-competent state of IL-1RAcP is selected (we refer to “conformational selection” at this stage), IL-1RAcP fine-tunes the relative position between the D2 and D3 domains and the rotation of each domain (we refer to “induced-fit” at this stage) to bind to different cytokine/primary receptor complexes to form higher affinity ternary complexes.

Our previous SAXS studies on ST2 and IL-1RAcP suggest that ST2 is highly flexible, whereas IL-1RAcP prefers to stay as a single conformation in solution (Liu et al., 2013). In this study, to confirm our previous conclusion we revisited the published data and performed comprehensive mass spectrometric analysis to map the glycans for building the full-atom model for SAXS analysis by more advanced SAXS modeling approach (Rambo and Tainer, 2011, Hammel, 2012, Rambo and Tainer, 2013, Remesh et al., 2018). The results of this study verified the distinct inter-domain flexibility of ST2 and the less flexible nature of IL-1RAcP.

Perturbed inter-domain conformational dynamics were also observed in the other co-receptor IL-18Rβ mutant with impaired binding and NF-κB signaling functions, whose D2/D3 linker was swapped with that of IL-18Rα. There is a notable difference between IL-1RAcP and IL-18Rβ regarding the inter-domain flexibility in the D1D2 module. All the solved crystal structures of IL-1RAcP can be superimposed according to the D1D2 module with the D3 domain rotating in different directions. A good fitting to the SAXS data (χ=1.05) was also achieved in the un-bound IL-1RAcP with flexible D2/D3 linker. By contrast, the SAXS fitting showed that the inter-domain flexibility of IL-18Rβ originated not only from the D2/D3 linker, but also from the D1/D2 linker. Interestingly, the crystal structure of IL-18/IL-18Rα-ECD/lL-18Rβ-ECD (PDB: 3W04) showed an opposite orientation of the D1 domain relative to the D2 domain in the D1D2 module of IL-18Rβ compared with IL-1RAcP (Tsutsumi et al., 2014). It was suggested that the unique D1/D2 orientation in IL-18Rβ might be a result of the lack of β-strand d2 that is typically conserved in other IL-1 receptors. However, the primary receptor IL-18Rα, which also lacks the β-strand d2, displayed a D1/D2 orientation similar to that of other primary receptors and IL-1RAcP. Therefore, the inter-domain flexibility in the D1D2 module may also account for

the unique D1/D2 orientation in IL-18Rβ when it participates in forming the ternary signaling complex.

Taken together, our results reveal the structure-dynamic relationships of IL-1 receptors and provided insights into the functional significance of linker flexibility for a better understanding of the solution behavior of IL-1 receptors. Moreover, IL-1 receptors are potential drug targets for modulating the activity of cytokines in cytokine-related pathological diseases (Dinarello, 2002, Sims and Smith, 2010). Because of no crystal structures of ligand free IL-1 receptors are available to date, the ensembles of IL-1 receptors showing the most relevant structures in solution are useful for the analysis of druggable sites and for virtual screening to predict suitable compounds that interact with each IL-1 receptor (Yang et al., 2016).

STAR METHODS

CONTACT FOR REAGENT AND RESOURCE SHARING

Further information and requests for resources and reagents should be directed to and will be fulfilled by the Lead Contacts -XQ.W. (xinquanwang@mail.tsinghua.edu.cn).

EXPERIMENTAL MODEL AND SUBJECT DETAILS

HEK 293T cells were cultured in DMEM with 10% fetal bovine serum (FBS) and incubated at 37 °C in a humidified atmosphere of 5% $C0_2$. For 293T-IL-1RAcP-KO cells, 1 μg/ml puromycin was added. Spodoptera frugiperda (sf9) insect cells were cultured in sf900 medium at 27°C, 110rpm. *Escherichia coli* BL21 (DE3) cells used for IL-1 cytokine expression were cultured in LB media; the cells were induced with 0.5 mM IPTG at 16°C for 18 h. *Sodoptera frugiperda* 9 (sf9) insect cells used for IL-1 receptor expression were cultured in SF900 medium at 27°C; the medium containing secreted proteins was collected with 48h post-infection.

METHOD DETAILS

Plasmid Construction—cDNA for human full-length ST2, IL-1RI, IL-1Rrp2, IL-1RAcP, IL-18Rα, and IL-18Rβ were cloned into pcDNA3.1(+) (Invitrogen). The corresponding extracellular domain (ECD) of these receptors were cloned into pFastBad1 (Invitrogen), with gp67 signal peptide in the N-terminal. The ectodomain was as listed: L18-V331 for IL-1RI-ECD; F14-V341 for IL-1RII-ECD; K19-K321 for ST2-ECD; S21-K350 for IL-1RAcP-ECD; C22-R329 for IL-18Rα-ECD; and F20-E354 for IL-18Rβ-ECD. Loop-swapped mutation were introduced by overlapping PCR. IL-33, IL-1β, pro-IL-18 and IL-36γ were cloned as previously (Wei et al., 2014, Wang et al., 2010, Liu et al., 2013). All the constructs were cloned by seamless ligation kit (Vazyme, Cat# C112-02). The sequences of all constructs were determined by DNA sequencing.

Protein Expression and Purification—All the cytokines, including IL-33, IL-1β, mature IL-18 and IL-36γ, were expressed in *Escherichia coli* BL21 (DE3) pLysS and purified as previously (Wei et al., 2014, Wang et al., 2010, Liu et al., 2013). All the ectodomains of IL-1 receptors, including ST2-ECD, IL-1RI-ECD, IL-1RII-ECD, IL-1RAcP-

ECD, IL-18Rα-ECD, IL-18Rβ-ECD and the D2/D3 linker replaced IL-1RAcP-ECD mutants were expressed in sf9 cells. Their detailed purification procedures were as described previously (Wei et al., 2014, Wang et al., 2010, Liu et al., 2013). The supernatant was collected 48h after transfection, then purified through Ni-NTA affinity chromatography and size-exclusion chromatography. The behavior and purity were verified by SAS-PAGE and size-exclusion chromatography. All the IL-1 receptors behave well except IL-1Rrp2-ECD with oligomeric state. For SAXS data collection, 3% (vol/vol) glycerol was added to the size-exclusion chromatography buffer to reduce the effects of radiation damage, assuming that the addition of glycerol does not affect the sample. To obtain the binary complex formed by cytokine and receptor, including IL-33/ST2-ECD, IL-1β/IL-1RI-ECD and IL-18/IL-18Rα-ECD, cytokine and receptor were mixed at a molar ratio of 1.2:1 for 2h at 4°C and further purify by size-exclusion chromatography.

Surface Plasmon Resonance Analysis—Kinetic parameters and affinities of protein-protein interactions were measured by SPR analysis using a BIAcore T200 instrument (GE Healthcare) at 25°C. IL-1RAcP-ECD or chimeric IL-1RAcP-ECD was immobilized on a research-grade CM5 sensor chip by amine-coupling method. Flow cell 1 was left blank as a reference. Approximately 150 response units of IL-1RAcP-ECD or chimeric IL-1RAcP-ECD (20 μmlg/ml) in sodium acetate buffer (10 mM; pH 5.0) was captured directly on the flow cell 2, and the surface was then blocked with an injection of 1 M ethanolamine (pH 8.0) for 7 min. For the collection of data for kinetic analysis, preformed binary complex of IL-33/ST2-ECD or IL-1β/IL-lRI-ECD in a buffer of 10 mM Hepes (pH 7.2), 150 mM NaCI, and 0.005% (vol/vol) Tween-20 was injected over the flow cells using five concentrations of a twofold titration series at a 30 μl/min flow rate. The ternary complex was allowed to associate for 60 s and dissociate for 180 s. The sensor surface was regenerated with 5 mM NaOH. The results was analyzed with BIAcore T200 evaluation software (GE Healthcare) by fitting to a 1:1 Langmuir binding fitting model. The direct immobilization of IL-18Rβ-ECD on the CM5 sensor chip will block its interaction with the preformed IL-18/IL-18Rα-ECD. All the procedures are the same for IL-18Rβ-ECD except that streptavidin was immobilized on the CM5 sensor chip first to capture the biotinylated IL-18Rβ-ECD.

***IL-1RAcP* Knockout in HEK 293T—**To generate IL-1RAcP knockout HEK293T cells, the Cas9 with a pair of sgRNAs were used. The guide sequence used are 5'-TGTGATCCATTCACCTAATG-3' and 5'-CATTAGGTGAATGGATCACA-3' for human IL-1RAcP targeting to Exon 6; 5'-CATGGTCTTCTTCTGCATTA-3' and 5'-CTCCGAGCGGATGTACCCCG-3' for mCherry as a control. sgRNAs were designed using the online sgRNA design tool available at https://crispr.mit.edu/. The corresponding sense and antisense DNA oligomers were annealed and cloned into BsmBI site of lentiCRISPRv2 (Invitrogen). Lentiviral particles were produced in HEK 293T cells by co-transfection of lentiviral vectors, packing plasmid psPAX2 (Addgene Cat# 12260) and envelope plasmid pMD2.G (Addgene Cat# 12259). The supernatant containing lentiviral particles was collected and used to infect HEK 293T in the presence of 8 μg/ml polybrene (Sigma-Aldrich). 48h later, HEK 293T cells were selected with 1 μg/ml puromycin (AMRESCO). Single cell was sorted by fluorescence-activated cell sorting (FACS). CRISPR/Cas9 induced mutations were analyzed on genomic DNA isolated from the generated KO clones as well as

from the parental cell lines and non-relevant control. At last, the knockout clones were validated by expression level analysis and dual-luciferase assay.

Dual-luciferase Reporter Assay—To measure the IL-1-mediated NF-κB signaling, cells were transiently transfected with full-length human IL-1 receptors cloned into pcDNA3.1. The full-length IL-1 receptors was modified with C726G synonymous mutation to escape Cas9 digestion. The human NF-κB-firefly luciferase was used as a reporter of IL-1 signaling. A constitutively active promoter was constructed just before Renilla luciferase to normalize the transfection efficiency. Cells were seeded in Costar White 24-well plates prior to transfection. For transfections, 100 ng receptors, 60 ng NF-κB-firefly luciferase gene and 5 ng Renilla luciferase reporter gene were mixed and transfected with PEI (1:3.5) per well. All transfections were amended with empty pcDNA3.1 to allow that equal amounts of plasmid were transfected. 12h after the transfection, the medium was replaced with fresh DMEM without FBS to starve the cells for another 12h. Then cells were incubated with titrated concentrations of IL-1 cytokines (1 nM IL-33, 1 nM IL-1 β, 25 nM IL-36γ; 6 nM IL-18) for 6h prior to cell lysis. The luciferase activity was measured using the dual-luciferase reporter kit (Vigorous bio) in the Centro LB960 plate reader. 120 μl 1 xlysis buffer was added to each well for 20 min at room temperature. After lysis, 20 μi lysate was transferred into the reading plate. The firefly luciferase activity was recorded as soon as substrate 1 was added. Then the Renilla luciferase activity was detected with substrate 2 added. All the procedures were protected from light. The signal of firefly luciferase was divided by that of Renilla luciferase to normalize the transfection efficiency. The data were plotted as fold induction of the firefly luciferase expressed from the NF-κB promoter relative to that of the cells expressing only the vector control. In addition, the corresponding lysate was used for western-blot to quantify the expression level. All the experiments were performed in triplicate.

Circular Dichroism—Circular dichroism measurements were conducted with Chirascan-plus CD Spectrometer (Applied Photophysics). All the data were collected with 0.25 mg/mL samples, including IL-1RAcP-ECD-WT, IL-18Rβ-ECD-WT as well as their D2/D3 linker exchanged mutants in 10 mM Hepes (pH 7.2), 150 mM NaCI buffer over a wavelength range of 190–260 nm, with 1 nm increments, in a 1 mm-pathlength rectangular cuvette at 25 °C. All the measurements were performed in triplicate.

Subcellular Fractionation—293T-IL-1RAcP-KO transfected with IL-1RAcP or IL-18Rβ were washed twice with ice-cold PBS. 500μl suspension buffer (10 mM Hepes, pH 7.2; 150 mM NaCI and protein inhibitor cocktail) per 10 cm-dish was added. Cell lysates were collected and transferred to a 1.5ml tube. The lysates were grinded with rod and centrifuged at 500×g for 10 min. Both cytoplasm and membrane fraction were contained in the supernatant. The supernatant then was ultra-centrifuged at 100,000×g for 1h. Cytoplasm was contained in supernatant and membrane fraction was contained in the pellet. The pellet was suspended in suspension buffer with 1% NP40 for 2h. Then the membrane fraction was extracted from membrane into supernatant. All the above procedures were done at 4 °C.

Western Blot—All the samples prepared for western blot are solubilized with 1× SDS/PAGE sample buffer (Invitrogen) with 5% β-mercaptoethanol (β-ME), without boiling, and separated with 10% Tris-glycine SDS/PAGE (Invitrogen). Following SDS/PAGE, proteins were transferred onto nitrocellulose membranes (Bio-Rad). For IL-1RAcP knockout, rabbit-anti-IL-1RAcP (Rockland) was used; for subcellular localization of IL-1RAcP, rabbit-anti-IL-1RAcP (ABCam) was used; for IL-18Rp, rabbit anti-flag tag (MBL) at c-terminus was used. Immunoblotting data was collected using AI600 (GE Health).

Small-angle X-ray-scattering (SAXS) Data Collection and Analysis—SAXS data were collected at the SIBLYS beamline 12.3.1 of the Advanced Light Source at the Lawrence Berkeley National Laboratory (Classen et al., 2013) at 1.03 A wavelength using a Pilatus 2M detector at 1.5 m sample-to-detector distance, resulting in scattering vectors ranging from 0.01 to 0.4 $Å^{-1}$. The scattering vector is defined as $q = 4\pi$ sinO/λλ, where 2θ is the scattering angle. Size exclusion chromatography in line with SAXS data collection (SEC-SAXS) was performed to ensure the aggregation free state of the sample. The SEC column (Schodex kw-803) was equilibrated with running buffer (10 mM Hepes, pH 7.2, 150 mM NaCI, 3% (vol/vol) glycerol, and 0.01% sodium azide) with a flow rate of 0.5 mL/min. 50 μl sample was run through SEC and 3 s X-ray exposures were collected continuously during a ~25 min elution. The SAXS frames recorded prior to the protein elution peak were used to subtract all other frames. R_g were determined based on the Guinier approximation $l(q) = l(0) \exp(-q^2R_g^2/3)$ (Guinier, 1955) with the limits $qR_g < 1.3$. Further, scattering intensity at q = 0 $Å^{-1}$ (l(0)) and R_g values were compared for each collected SAXS curve across the entire elution peak. The elution peak was mapped by plotting the scattering intensity at q=0 $Å^1$ (I(0)) relative to the recorded frame. SAXS was also acquired in the high throughout modality (HT-SAXS) (Hura et al., 2009) at sample concentrations between 1-5 mg/mL to compare with SEC-SAXS profile. The interference-free SAXS curves were merged and analyzed by program SCATTER. Pair distribution function P(r) was computed by program GNOM (Konig, Svergun, Koch, Hubner, & Schellenberger, 1992).

Solution Structure Modelling—The crystal structure of IL-1RAcP-ECD (4DEP:C), IL-1RI-ECD (4DEP:B), IL-1RII -ECD (3040:C), ST2-ECD (4KC3:B), IL-18Rα-ECD (3W04:B) and IL-18Rβ-ECD (3W04:C) were used as initial models. The missing residues and linkers were generated by program MODELLER (Sali and Blundell, 1993). The glycosylated models were built by using the web server CHARMM-GUI (Brooks et al., 2009), in which the full-atomic protein PDB structural files were input and the glycans determined from mass spectrometry were added by “Glycan Reader & Modeler” functional modules in CHARMM-GUI. The full-atomic glycosylated model is generated with parameterized output files for BILBOMD. The glycosylated models were subsequently input to BILBOMD (Pelikan et al., 2009) to explore the conformational space adopted by D3 domain. The theoretical SAXS profile and the corresponding fit to the experimental data were calculated using the program FoXS (Schneidman-Duhovny et al., 2013). MultiFoXS (Schneidman-Duhovny et al., 2016) was used to identify the multistate model of the receptors coexisting in solution to best fit the experimental SAXS profile. The structures were visualized in CHIMERA (Pettersen et al., 2004).

Mass spectrometry—Glycopeptide mapping was performed on the native and deglycosylated proteins (PNGase F new England biolabs) with trypsin and chymotrypsin digestion as follows. For denaturation 25 μl of each protein (1 mg/mL) was diluted with 75 μl of 8M Guanidine HCI buffered at pH 8.0 and mixed. Next reduction was carried out by adding 2.5 μl of thawed aliquot of 1 M DTT (Sigma 43816-10ML, BioUltra) followed by incubation for 1 hour at 37 °C. Alk ylation with 6 μl of 1 M iodoacetamide solution (Sigma, A3221-10VL) was performed in the dark followed by quenching with 3.75 μl of 1 M DTT (Sigma 43816-10ML, BioUltra) to quench unreacted iodoacetamide. The samples were then desalted using Zeba Spin Desalting columns (ThermoFisher Scientific) according to the manufacturer's protocol in 100 mM Ammonium Bicarbonate, 1mM $CaCI_2$, pH=7.0 (digestion buffer). The samples were then digested with trypsin or chymotrypsin (Promega sequencing grade, final concentration of 0.2 μg/μl of enzyme freshly reconstituted in 50 mM acetic acid) for 4h at 37 °C. Digestion was quenched with 1 μl of 100% trifluoroscetic acid. Approximately 15 μl of the digested protein sample (~ 3 μg of digested product) was injected on a Agilent Zorbax SB-C18 Rapid Resolution HD (2.1 × 150mm 1.8 micron) using an autosampler at a flow rate of 0.3 mL/min. The column was kept at 60 °C. Mass spectrometry gra de HPLC solvents used were - Mobile phase A: 0.1% formic acid/water (Chromasolv Honeywell LCMS grade) and mobile phase B: 0.1% formic acied/acetonitrile (Chromasolv, LC-MS grade). The column effluent was introduced into a Thermofisher Q-Exactive Orbitrap mass spectrometer via electrospray ionization using a capillary voltage of 2.5 kV. The glycopeptide map was processed using Protein Metrics Byonic^{TM} software to determine glycan composition at each site.

QUANTIFICATION AND STATISTICAL ANALYSIS

Details about the sample size and statistical analysis of the different experiments can be found in each methods section. In general, we used single protein samples for SAXS studies and mass spectrometry, while surface plasmon resonance analysis, *IL-1RAcP* knockout, signaling studies and subcellular fractionation were performed at least three independent experiments. Furthermore, for signaling studies mean αS.D. was plotted. Origin 9.1 was used for data plotting.

DATA AND SOFTWARE AVAILABILITY

SAXS data were deposited in the Small Angle Scattering Biological Data Bank (SASBDB). The accession codes are SASDE59 (IL-1RI-ECD), SASDE69 (IL-1RII-ECD), SASDE79 (IL-18Rα-ECD), SASDEZ8 (IL-18Rβ-ECD), SASDE29 (IL-1RAcP-ECD-RI), SASDE89 (IL-1RAcP-ECD-RII), SASDE49 (IL-1RAcP-ECD-ST2), SASDE39 (IL-18Rβ-ECD-18Rα). All software used for the modeling studies are open-source and can be downloaded from websites as indicated in the Key Resource Table.

Supplementary Material

Refer to Web version on PubMed Central for supplementary material.

ACKNOWLEDGMENTS

We sincerely thank Professors Xianyang Fang (Tsinghua University), Haipeng Gong (Tsinghua University), Xinqi Gong (Renmin University) and Dr. Meng Ke for helpful discussions. This work was conducted at the Advanced Light Source (ALS), a national user facility operated by Lawrence Berkeley National Laboratory on behalf of the Department of Energy, Office of Basic Energy Sciences, through the Integrated Diffraction Analysis Technologies (IDAT) program, supported by DOE Office of Biological and Environmental Research. Additional support comes from the National Institutes of Health project ALS-ENABLE (P30 GM124169) and a High-End Instrumentation Grant S100D018483. We thank Jinquan Luo of Janssen R&D supported this work for collecting and analyzing mass spectroscopic data. This work was supported by the National Natural Science Foundation of China (31470751 and U1405228) and the National Key Plan for Scientific Research and Development of China (2016YFD0500307) to Xinquan Wang, and also supported by the Ministry of Science and Technology, R.O.C. (103-2311-B-006-006 and 104-2320-B-006-050) to Shuying Wang.

REFERENCES

Adachi O, Kawai T, Takeda K, Matsumoto M, Tsutsui H, Sakagami M, Nakanishi K & Akira S 1998 Targeted disruption of the MyD88 gene results in loss of IL-1-and IL-18-mediated function. Immunity 9, 143–150. [PubMed: 9697844]

Bernado P, Mylonas E, Petoukhov MV, Blackledge M & Svergun DI 2007 Structural characterization of flexible proteins using small-angle X-ray scattering. J. Am. Chem. Soc. 129, 5656–5664. [PubMed: 17411046]

Bernado P & Svergun DI 2012 Structural analysis of intrinsically disordered proteins by small-angle X-ray scattering. Mol. Biosyst. 8, 151–167. [PubMed: 21947276]

Born TL, Smith DE, Garka KE, Renshaw BR, Bertles JS & Sims JE 2000 Identification and characterization of two members of a novel class of the interleukin-1 receptor (IL-1 R) family. Delineation Of a new class of IL-1R-related proteins based on signaling. J. Biol. Chem. 275, 41528.

Bowie A & O'neill L. a. J. 2000 The interleukin-1 receptor/Toll-like receptor superfamily: signal generators for pro-inflammatory interleukins and microbial products. Journal of Leukocyte Biology 67, 508–514. [PubMed: 10770283]

Brooks BR, Brooks CL 3rd, Mackerell AD Jr., Nilsson L, Petrella RJ, Roux B, Won Y, Archontis G, Bartels C, Boresch S, Caflisch A, Caves L, Cui Q, Dinner AR, Feig M, Fischer S, Gao J, Hodoscek M, Im W, Kuczera K, Lazaridis T, Ma J, Ovchinnikov V, Paci E, Pastor RW, Post CB, Pu JZ, Schaefer M, Tidor B, Venable RM, Woodcock HL, Wu X, Yang W, York DM & Karplus M 2009 CHARMM: the biomolecular simulation program. J. Comput. Chem. 30, 1545–1614. [PubMed: 19444816]

Bruning JB, Parent AA, Gil G, Zhao M, Nowak J, Pace MC, Smith CL, Afonine PV, Adams PD, Katzenellenbogen JA & Nettles KW 2010 Coupling of receptor conformation and ligand orientation determine graded activity. Nat. Chem. Biol. 6, 837–843 [PubMed: 20924370]

Colotta F, Re F, Muzio M, Bertini R, Polentarutti N, Sironi M, Giri JG, Dower SK, Sims JE & Mantovani A 1993 Interleukin-1 type II receptor: a decoy target for IL-1 that is regulated by IL-4. Science 261, 472–475. [PubMed: 8332913]

Cullinan EB, Kwee L, Nunes R, Shuster DJ, Ju G, Mcintyre KW, Chizzonite RA & Labow MA 1998 IL-1 receptor accessory protein is an essential component of the IL-1 receptor. J. Immunol. 161, 5614–5620. [PubMed: 9820540]

Debets R, Timans JC, Homey B, Zurawski S, Sana TR, Lo S, Wagner J, Edwards G, Clifford T, Menon S, Bazan JF & Kastelein RA 2001 Two novel IL-1 family members, IL-1 delta and IL-1 epsilon, function as an antagonist and agonist of NF-kappa B activation through the orphan IL-1 receptor-related protein 2. J. Immunol. 167, 1440–1446. [PubMed: 11466363]

Dinarello CA 2002 The IL-1 family and inflammatory diseases. Clin. Exp. Rheumatol. 20, S1–13.

Ferofontov A, Strulovich R, Marom M, Giladi M & Haitin Y 2018 Inherent flexibility of CLIC6 revealed by crystallographic and solution studies. Sci. Rep. 8, 6882. [PubMed: 29720717]

Galburt EA & Tomko EJ 2017 Conformational selection and induced fit as a useful framework for molecular motor mechanisms. Biophysical Chemistry 223, 11–16. [PubMed: 28187350]

Garlanda C, Dinarello CA & Mantovani A 2013a The interleukin-1 family: back to the future. Immunity 39, 1003–1018. [PubMed: 24332029]

Garlanda C, Riva F, Bonavita E & Mantovani A 2013b Negative regulatory receptors of the IL-1 family. Semin Immunol. 25, 408–415. [PubMed: 24239046]

Jo S, Kim T, Iyer VG & Im W 2008 CHARMM-GUI: a web-based graphical user interface for CHARMM. J. Comput. Chem. 29, 1859–1865. [PubMed: 18351591]

Gunasekaran K, Ma BY & Nussinov R 2004 Is allostery an intrinsic property of all dynamic proteins. Proteins-Structure Function and Bioinformatics, 57, 433–443.

Gunther S, Deredge D, Bowers AL, Luchini A, Bonsor DA, Beadenkopf R, Liotta L, Wintrode PL & Sundberg EJ 2017 IL-1 Family Cytokines Use Distinct Molecular Mechanisms to Signal through Their Shared Co-receptor. Immunity 47, 510–523 e4. [PubMed: 28930661]

Hammel M 2012 Validation of macromolecular flexibility in solution by small-angle X-ray scattering (SAXS). Eur. Biophys. J. 41, 789–799. [PubMed: 22639100]

Huang J, Gao X, Li S & Cao Z 1997 Recruitment of IRAK to the interleukin 1 receptor complex requires interleukin 1 receptor accessory protein. Proc. Natl. Acad. Sci. USA, 94, 12829–12832. [PubMed: 9371760]

Jo S, Kim T, Iyer VG & Im W 2008 CHARMM-GUI: a web-based graphical user interface for CHARMM. J. Comput. Chem. 29, 1859–1865. [PubMed: 18351591]

Koshland DE 1958 Application of a Theory of Enzyme Specificity to Protein Synthesis. Proc. Natl. Acad. Sci. USA, 44, 98–104. [PubMed: 16590179]

Liu X, Hammel M, He Y, Tainer JA, Jeng US, Zhang L, Wang S & Wang X 2013 Structural insights into the interaction of IL-33 with its receptors. Proc. Natl. Acad. Sci. USA 110, 14918–14923. [PubMed: 23980170]

Matoba K, Mihara E, Tamura-Kawakami K, Miyazaki N, Maeda S, Hirai H, Thompson S, Iwasaki K & Takagi J 2017 Conformational Freedom of the LRP6 Ectodomain Is Regulated by N-glycosylation and the Binding of the Wnt Antagonist Dkk1. Cell Rep. 18, 32–40. [PubMed: 28052259]

Mcmahan CJ, Slack JL, Mosley B, Cosman D, Lupton SD, Brunton LL, Grubin CE, Wignall JM, Jenkins NA, Brannan CI & et al. 1991 A novel IL-1 receptor, cloned from B cells by mammalian expression, is expressed in many cell types. EMBO J. 10, 2821–2832. [PubMed: 1833184]

Nussinov R, Ma B & Tsai CJ 2014 Multiple conformational selection and induced fit events take place in allosteric propagation. Biophys. Chem. 186, 22–30. [PubMed: 24239303]

O'neill LA 2008a The interleukin-1 receptor/Toll-like receptor superfamily: 10 years of progress. Immunol. Rev. 226, 10–18. [PubMed: 19161412]

Palomo J, Dietrich D, Martin P, Palmer G & Gabay C 2015 The interleukin (IL)-1 cytokine family--Balance between agonists and antagonists in inflammatory diseases. Cytokine 76, 25–37. [PubMed: 26185894]

Pelikan M, Hura GL & Hammel M 2009 Structure and flexibility within proteins as identified through small angle X-ray scattering. Gen. Physiol. Biophys. 28, 174–189.

Pettersen EF, Goddard TD, Huang CC, Couch GS, Greenblatt DM, Meng EC & Ferrin TE 2004 UCSF chimera - A visualization system for exploratory research and analysis. J. Comput. Chem. 25, 1605–1612. [PubMed: 15264254]

Polentarutti N, Rol GP, Muzio M, Bosisio D, Camnasio M, Riva F, Zoja C, Benigni A, Tomasoni S, Vecchi A, Garlanda C & Mantovani A 2003 Unique pattern of expression and inhibition of IL-1 signaling by the IL-1 receptor family member TIR8/SIGIRR. Eur. Cytokine Netw. 14, 211–218. [PubMed: 14715412]

Puz V, Pavsic M, Lenarcic B & Djinovic-Carugo K 2017 Conformational plasticity and evolutionary analysis of the myotilin tandem Ig domains. Sci. Rep. 7, 3993. [PubMed: 28638118]

Qin J, Qian Y, Yao J, Grace C & Li X 2005 SIGIRR inhibits interleukin-1 receptor- and toll-like receptor 4-mediated signaling through different mechanisms. J. Biol. Chem. 280, 25233–25241. [PubMed: 15866876]

Rambo RP & Tainer JA 2011 Characterizing flexible and intrinsically unstructured biological macromolecules by SAS using the Porod-Debye law. Biopolymers 95, 559–571. [PubMed: 21509745]

Rambo RP & Tainer JA 2013 Accurate assessment of mass, models and resolution by small-angle scattering. Nature 496, 477–481. [PubMed: 23619693]

Remesh SG, Armstrong AA, Mahan AD, Luo J & Hammel M 2018 Conformational Plasticity of the Immunoglobulin Fc Domain in Solution. Structure 26, 1007–1014 e2. [PubMed: 29731233]

Ruiz DM, Turowski VR & Murakami MT 2016 Effects of the linker region on the structure and function of modular GH5 cellulases. Sci. Rep. 6, 28504. [PubMed: 27334041]

Sali A & Blundell TL 1993 Comparative Protein Modeling by Satisfaction of Spatial Restraints. Journal of Molecular Biology 234, 779–815. [PubMed: 8254673]

Sanjana NE, Shalem O & Zhang F 2014 Improved vectors and genome-wide libraries for CRISPR screening. Nat. Methods 11, 783–784. [PubMed: 25075903]

Schneidman-Duhovny D & Hammel M 2018 Modeling Structure and Dynamics of Protein Complexes with SAXS Profiles. Methods Mol. Biol. 1764, 449–473. [PubMed: 29605933]

Schneidman-Duhovny D, Hammel M, Tainer JA & Sali A 2013 Accurate SAXS Profile Computation and its Assessment by Contrast Variation Experiments. Biophysical Journal 105, 962–974. [PubMed: 23972848]

Schneidman-Duhovny D, Hammel M, Tainer JA & Sali A 2016 FoXS, FoXSDock and MultiFoXS: Single-state and multi-state structural modeling of proteins and their complexes based on SAXS profiles. Nucleic Acids Res. 44, W424–429. [PubMed: 27151198]

Shalem O, Sanjana NE, Hartenian E, Shi X, Scott DA, Mikkelson T, Heckl D, Ebert BL, Root DE, Doench JG & Zhang F 2014 Genome-scale CRISPR-Cas9 knockout screening in human cells. Science 343, 84–87. [PubMed: 24336571]

Sims JE & Smith DE 2010 The IL-1 family: regulators of immunity. Nat. Rev. Immunol. 10, 89–102. [PubMed: 20081871]

Thayer KM, Lakhani B & Beveridge DL 2017 Molecular Dynamics-Markov State Model of Protein Ligand Binding and Allostery in CRIB-PDZ: Conformational Selection and Induced Fit. J. Phys. Chem. B 121, 5509–5514. [PubMed: 28489401]

Thomas C, Bazan JF & Garcia KC 2012 Structure of the activating IL-1 receptor signaling complex. Nat Struct. Mol. Biol. 19, 455–457. [PubMed: 22426547]

Tossavainen H, Raulinaitis V, Kauppinen L, Pentikainen U, Maaheimo H & Permi P 2018 Structural and Functional Insights Into Lysostaphin-Substrate Interaction. Front. Mol. Biosci. 5, 60. [PubMed: 30018958]

Towne JE, Garka KE, Renshaw BR, Virca GD & Sims JE 2004 Interleukin (IL)-1 F6, IL-1 F8, and IL-1 F9 signal through IL-1 Rrp2 and IL-1 RAcP to activate the pathway leading to NF-kappaB and MAPKs. J. Biol. Chem. 279, 13677–13688. [PubMed: 14734551]

Towne JE, Renshaw BR, Douangpanya J, Lipsky BP, Shen M, Gabel CA & Sims JE 2011 Interleukin-36 (IL-36) ligands require processing for full agonist (IL-36alpha, IL-36beta, and IL-36gamma) or antagonist (IL-36Ra) activity. J. Biol. Chem. 286, 42594–42602. [PubMed: 21965679]

Tsutsumi N, Kimura T, Arita K, Ariyoshi M, Ohnishi H, Yamamoto T, Zuo X, Maenaka K, Park EY, Kondo N, Shirakawa M, Tochio H & Kato Z 2014 The structural basis for receptor recognition of human interleukin-18. Nat. Commun. 5, 5340. [PubMed: 25500532]

Wald D, Qin J, Zhao Z, Qian Y, Naramura M, Tian L, Towne J, Sims JE, Stark GR & Li X 2003 SIGIRR, a negative regulator of Toll-like receptor-interleukin 1 receptor signaling. Nat. Immunol. 4, 920–927. [PubMed: 12925853]

Wang D, Zhang S, Li L, Liu X, Mei K & Wang X 2010 Structural insights into the assembly and activation of IL-1betawith its receptors. Nat. Immunol, 11, 905–911. [PubMed: 20802483]

Wei H, Wang D, Qian Y, Liu X, Fan S, Yin HS & Wang X 2014 Structural basis for the specific recognition of IL-18 by its alpha receptor. FEBS Lett. 588, 3838–3843. [PubMed: 25261253]

Wriggers W, Chakravarty S & Jennings PA 2005 Control of protein functional dynamics by peptide linkers. Biopolymers 80, 736–746. [PubMed: 15880774]

Yang CY, Delproposto J, Chinnaswamy K, Brown WC, Wang S, Stuckey JA & Wang X 2016 Conformational Sampling and Binding Site Assessment of Suppression of Tumorigenicity 2 Ectodomain. PLoS One 11, e0146522. [PubMed: 26735493]

Ye L, Van Eps N, Zimmer M, Ernst OP & Prosser RS 2016 Activation of the A2A adenosine G-protein-coupled receptor by conformational selection. Nature 533, 265–268. [PubMed: 27144352]

Highlights

1. Family of IL-1 receptors possess inherent inter-domain flexibility
2. Altered inter-domain dynamics of IL-1 co-receptors results in loss of function
3. The natural D2/D3 linker is a critical functional determinant of IL-1 co-receptors

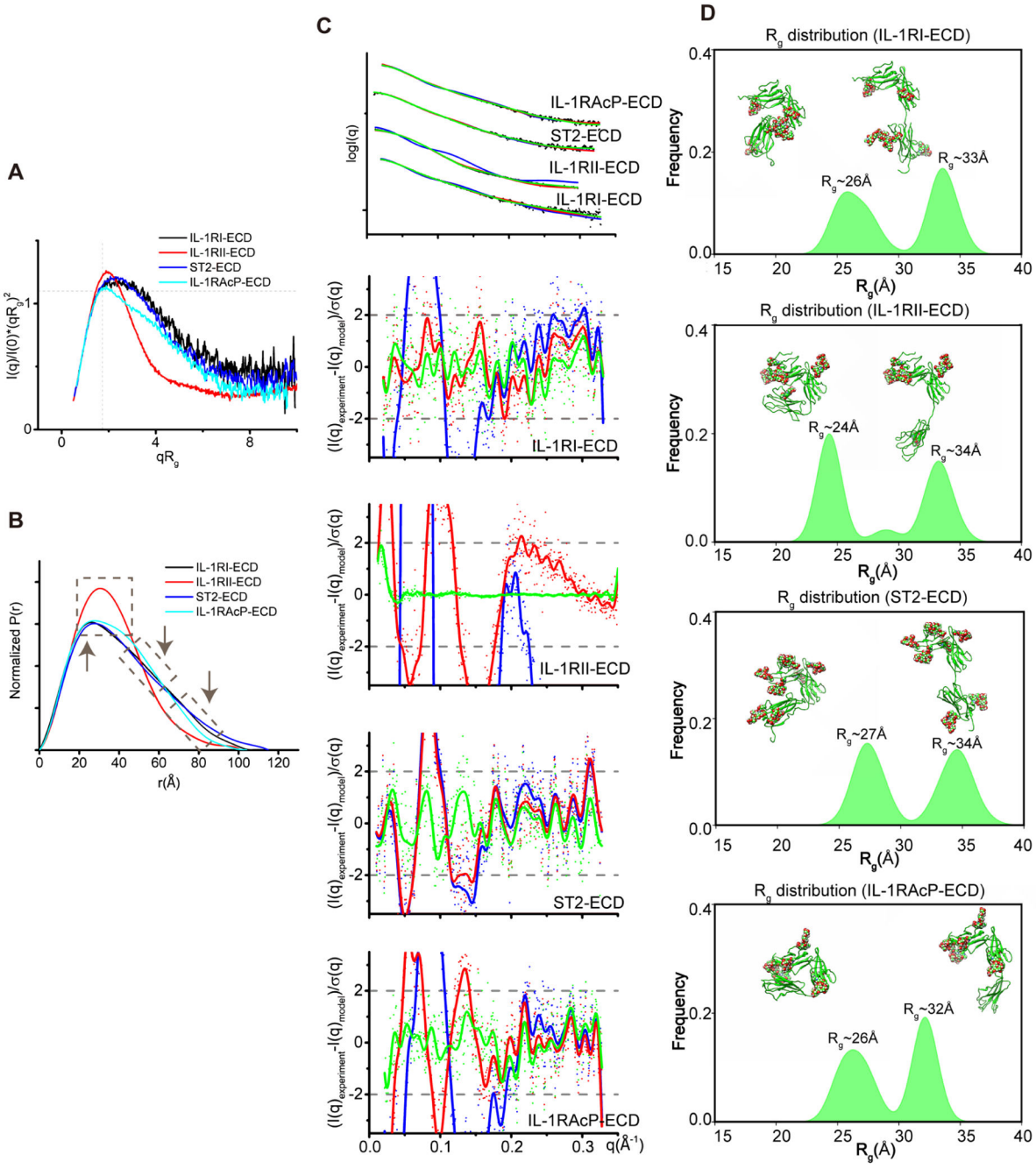

Figure 1. Flexibility and Conformational Ensemble of IL-1 Receptors by SAXS Analysis.

(A) Normalized Kratky plot of IL-1RI-ECD (black), IL-1RII-ECD (red), ST2-ECD (blue) and IL-1RAcP-ECD (cyan). IL-1RII-ECD (red) showed a bell-shaped plot, indicating a structure that is less flexible. (B) Normalized pair distribution function P(r) of IL-1RI-ECD (black), IL-1RII-ECD (red), ST2-ECD (blue) and IL-1RAcP-ECD (cyan). The q-range used for P(r) calculations is as follows: IL-1 RI-ECD (0.01730.2758Å^{-1}); IL-1RII-ECD (0.0142 to 0.2634 Å^{-1}); ST2-ECD (0.0125 to 0.2770 Å^{-1}); IL-1RAcP-ECD (0.0240 to 0.2946 Å^{-1}). The dotted rectangles indicate the different features between IL-1 receptors. (C) Fitting of

experimental data (black dots) to the theoretical profiles of the initial (blue), the best-fit (red) and ensemble model (green) of IL-1RI-ECD, IL-1RII-ECD, ST2-ECD and IL-1RAcP-ECD (up panel). Error-weighted residuals of the fitting after FFT smoothing (lines) (low panel). (D) The weighted R_g distribution of selected 100 two-state ensembles of IL-1RI-ECD, IL-1RII-ECD, ST2-ECD, and IL-1RAcP-ECD. The top two-state ensemble fitting the experimental data is shown as cartoon for visualization (glycans are shown as spheres). The peak height reflects the weight of the conformational state. (See also Figures S2 and S3, Table S1, Table S2 and Table S3)

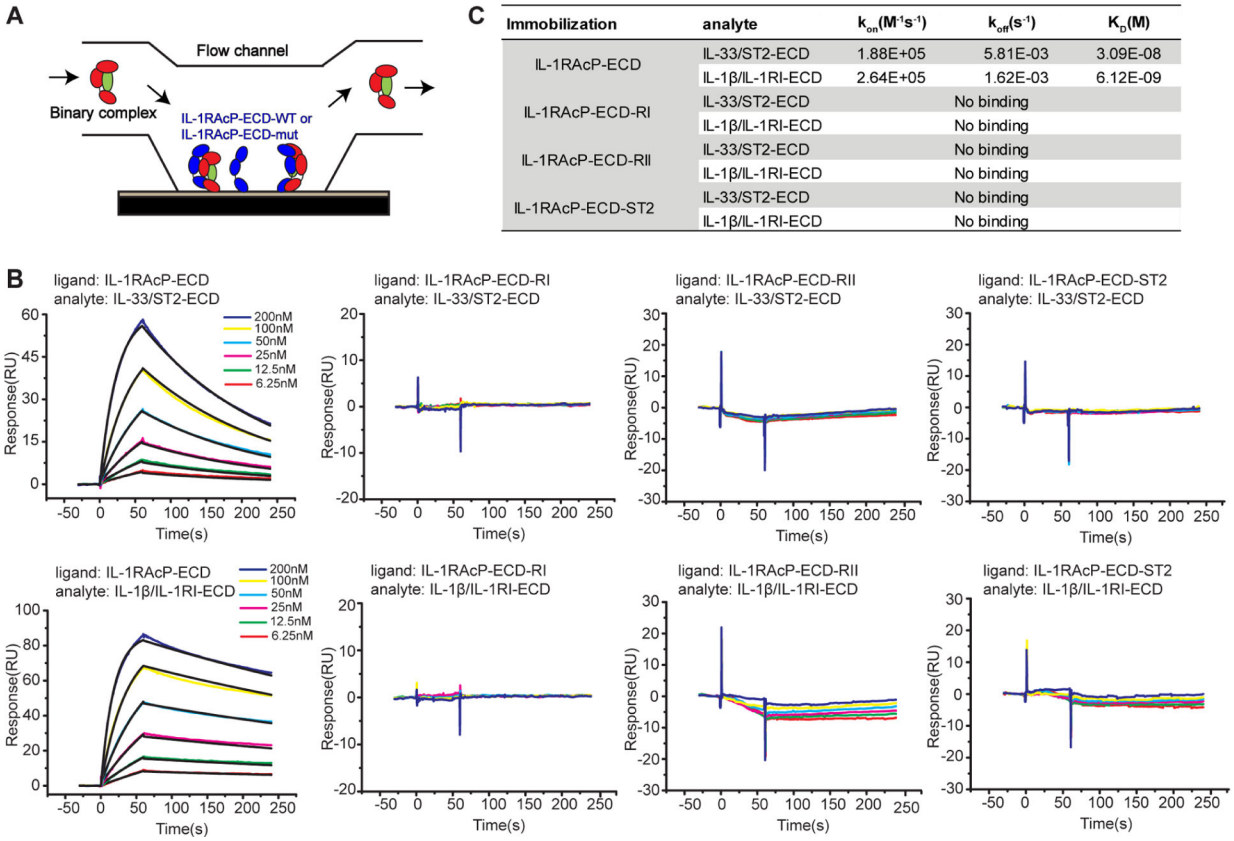

C

Immobilization	analyte	k_{on}($M^{-1}s^{-1}$)	k_{off}(s^{-1})	K_D(M)
IL-1RAcP-ECD	IL-33/ST2-ECD	1.88E+05	5.81E-03	3.09E-08
	IL-1β/IL-1RI-ECD	2.64E+05	1.62E-03	6.12E-09
IL-1RAcP-ECD-RI	IL-33/ST2-ECD	No binding		
	IL-1β/IL-1RI-ECD	No binding		
IL-1RAcP-ECD-RII	IL-33/ST2-ECD	No binding		
	IL-1β/IL-1RI-ECD	No binding		
IL-1RAcP-ECD-ST2	IL-33/ST2-ECD	No binding		
	IL-1β/IL-1RI-ECD	No binding		

Figure 2. SPR Analysis of the Binding of the D2/D3 Linker-replaced IL-1RAcP-ECD Mutants to the Binary Cytokine/Receptor Complex.

(A) Schematic presentation of the binding affinity measurement. Ligand: IL-1RAcP-ECD or D2/D3 linker-replaced IL-1RAcP-ECD mutants (IL-1RAcP-ECD-RI, IL-1RAcP-ECD-RII, IL-1RAcP-ECD-ST2); Analyte: the preformed binary complex IL-33/ST2-ECD or IL-1β/IL-1RI-ECD. (B) The binding of wild-type or mutated IL-1RAcP-ECD to the preformed binary complexes IL-33/ST2-ECD (up panel) and IL-1β/IL-1 RI-ECD (low panel). The SPR sensorgrams (black line) were fitted to a 1:1 Langmuir binding model (colored lines). (C) Comparison of the binding affinity of wild-type and D2/D3 linker-replaced IL-1RAcP-ECD. On rate (k_{on}), off rate (k_{off}) and dissociation constant (K_D) for the binding of IL-1RAcP-ECD and IL-1RAcP-ECD mutants to IL-33/ST2-ECD or IL-1β/IL-1RI-ECD were summarized. (See also Figure S1 and S5A)

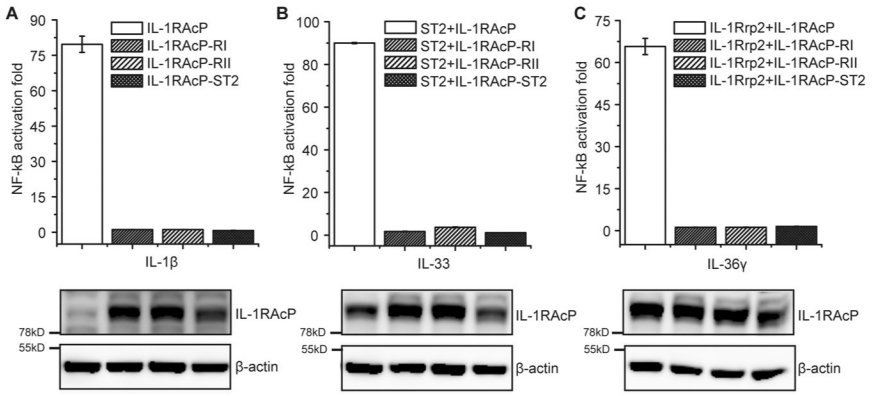

Figure 3. Effect of D2/D3 Linker Substitution within IL-1RAcP on IL-1 Signal Transduction.

The signal of NF-κB activation was measured in 293T-IL-1RAcP-KO cells, which were stimulated for 6h with IL-1 cytokines, including IL-1β (A), IL-33 (B), and IL-36γ (C) with the co-transfection of the respective primary receptors, IL-1RAcP or D2/D3 linker-replaced IL-1RAcP, and luciferase reporter genes. For IL-1β-mediated NF-κB signaling, only IL-1RAcP was transfected because of endogenous expression of IL-1Rl. The presented results are the means αS.D. from triplicate experiments. The protein levels of various IL-1RAcP were detected by western blot analysis with the whole cell lysate. The experiments were performed independently at least three times. (See also Figures S4 and S5C)

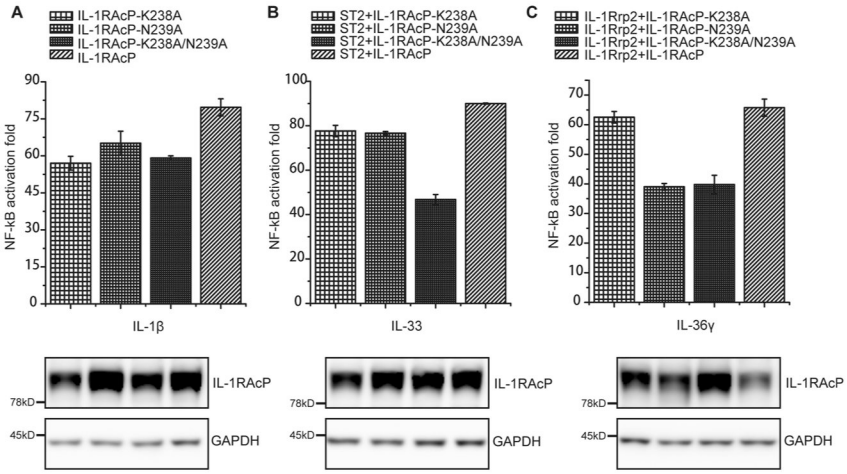

Figure 4. The Effect of Mutating the Contacting Residues K238 and N239 in IL-1RAcP D2/D3 Linker on IL-1 Signal Transduction.

The signal of NF-κB activation was measured in 293T-IL-1RAcP-KO cells upon stimulation with IL-1β (A), IL-33 (B) and IL-36γ (C), by co-transfection of primary receptors with IL-1RAcP, IL-1 $RAcP_{K238A}$, IL-1 $RAcP_{D239A}$ or IL-1$RAcP_{K238A/D239A}$ using the dual luciferase reporter assay. The presented results are the means αS.D.from triplicate experiments. The consistency of protein levels of mutated IL-1RAcP was confirmed by western blot analysis with the whole cell lysis. The experiments were performed independently at least three times. (See also Figures S4, S5C and S6)

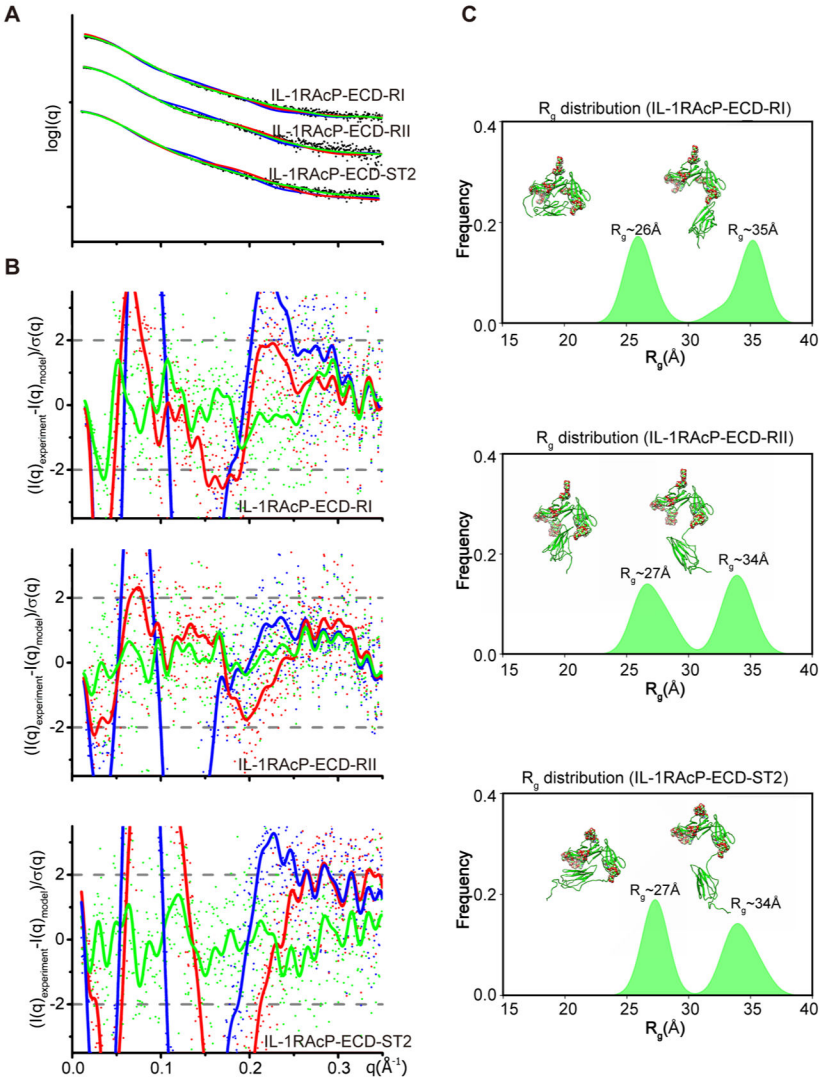

Figure 5. Altered Dynamics of D2/D3 Linker-replaced IL-1RAcP-ECD Mutants by SAXS Analysis.

(A) Fitting of the experimental data (black dots) to the theoretical profiles of the initial (blue), the best-fit (red) and ensemble model (green) of D2/D3 linker replaced IL-1RAcP mutants. (B) Error-weighted residuals of the fitting after FFT smoothing (lines). (C) The weighted R_g distribution of selected 100 two-state ensembles of D2/D3 linker-replaced IL-1 RAcP-ECD mutants. The top two-state ensemble fitting the experimental data is shown as cartoon for visualization (glycans are shown as spheres). The D1D2 module was in the same orientation as that of wild-type IL-1RAcP-ECD, while the D3 domain was rotated in a different orientation. The peak height reflects the weight of the conformational state and reveals the difference between wild-type IL-1RAcP-ECD and the mutants. (See also Figures S2 and S3, Table S1, Table S2 and Table S3)

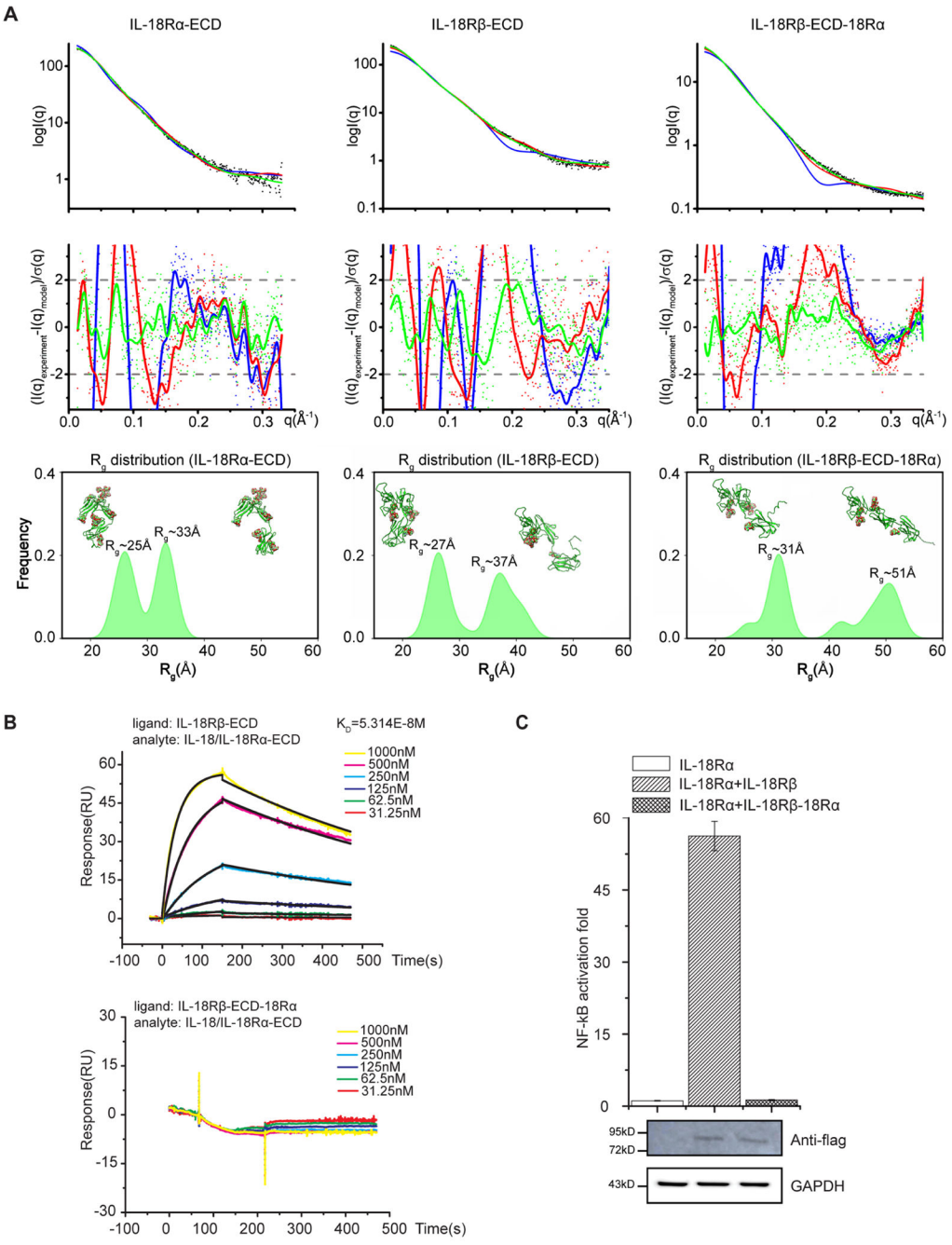

Figure 6. The Flexibility-dependent Function of IL-18Rβ-ECD.

(A) Flexibility assessment and conformational ensemble of IL-18Rα-ECD (up, left), IL-18Rβ-ECD (up, middle) and IL-18Rβ-ECD-18Rα (up, right). Error-weighted residuals of the fitting after FFT smoothing (lines) in the middle. The weighted R_g distribution of selected 100 two-state ensembles of IL-18 receptors. The top two-state ensemble fitting the experimental data is shown as cartoon for visualization (glycans are shown as spheres). (B) SPR analysis of the D2/D3 linker-replaced IL-18Rβ-ECD-18Rα mutants. (C) Effect of D2/D3 linker substitution in IL-18Rβ on IL-18-mediated NF-κB signaling assessed using the dual-luciferase reporter assay. The presented results are the means αS.D. from triplicate

experiments. The consistent protein level of mutated IL-18Rβ was detected by western blot analysis with the whole cell lysis. The experiments were performed independently at least three times. (See also Figures S1, S2, S3 and S5, Table S1, Table S2 and Table S3)

KEY RESOURCES TABLE

REAGENT or RESOURCE	SOURCE	IDENTIFIER
Antibodies		
Rabbit Anti-IL-1RAcP Antibody	Rockland	Cat# 600–401-BV3; RRID:AB_2613201
Rabbit Anti-IL-1RAcP Antibody	ABCam	Cat# ab8109, RRID:AB_306279
Mouse Monoclonal Anti-flag Antibody	MBL	Cat# M185–3L; RRID:AB_11123930
Mouse Monoclonal Anti-tubulin Antibody	Cell Signaling Technology	Cat# 3873; RRID:AB_1904178
Mouse Monoclonal Anti-β-actin Antibody	HuaXing Bio	Cat# HX1827
Mouse Monoclonal Anti-GAPDH Antibody	HuaXing Bio	Cat# HX1828
Chemicals, Peptides, and Recombinant Proteins		
polybrene	macgene	Cat# MC032
puromycin	AMRESCO	Cat# J593
dual-luciferase reporter kit	Vigorous biotechnology	Cat# T002
IL-1β	Wang et al., 2010	https://www.nature.com/articles/ni.1925
IL-33	Liu et al., 2013	https://www.pnas.org/content/110/37/14918.long
IL-36γ	This paper	N/A
IL-18	Wei et al., 2014	https://febs.onlinelibrary.wiley.com/doi/full/10.1016/j.febslet.2014.09.019
IL-1RI-ECD	Thomas et al., 2012	https://www.nature.com/articles/nsmb.2260
IL-1RII-ECD	Wang et al., 2010	https://www.nature.com/articles/ni.1925
ST2-ECD	Liu et al., 2013	https://www.pnas.org/content/110/37/14918.long
IL-1RAcP-ECD	Wang et al., 2010	https://www.nature.com/articles/ni.1925
IL-18Rα-ECD	Wei et al., 2014	https://febs.onlinelibrary.wiley.com/doi/full/10.1016/j.febslet.2014.09.019
IL-18Rβ-ECD	Tsutsumi et al., 2014	https://www.nature.com/articles/ncomms6340
IL-1RAcP-ECD-RI	This paper	N/A
IL-1RAcP-ECD-RII	This paper	N/A
IL-1RAcP-ECD-ST2	This paper	N/A
IL-18Rβ-ECD-18Rα	This paper	N/A
Deposited Data		
IL-1RI-ECD	Small Angle Scattering Biological Data Bank	SASDE59
IL-1RII-ECD	Small Angle Scattering Biological Data Bank	SASDE69
IL-18Rα-ECD	Small Angle Scattering Biological Data Bank	SASDE79
IL-18Rβ-ECD	Small Angle Scattering Biological Data Bank	SASDEZ8
IL-1RAcP-ECD-RI	Small Angle Scattering Biological Data Bank	SASDE29
IL-1RAcP-ECD-RII	Small Angle Scattering Biological Data Bank	SASDE89

REAGENT or RESOURCE	SOURCE	IDENTIFIER
IL-1RAcP-ECD-ST2	Small Angle Scattering Biological Data Bank	SASDE49
IL-18Rβ-ECD-18Rα	Small Angle Scattering Biological Data Bank	SASDE39
Experimental Models: Cell Lines		
IL-1RAcP-KO-293T	This paper	N/A
Spodoptera frugiperda (sf9)	ATCC	Cat# CRL-1711; RRID:CVCL_0549
Oligonucleotides		
sgRNA targeting human *IL-1RAcP* 5'-TGTGATCCATTCACCTAATG-3'	This paper	N/A
sgRNA targeting human *IL-1RAcP* 5'-CATTAGGTGAATGGATCACA-3'	This paper	N/A
sgRNA targeting mCherry 5'-CATGGTCTTCTTCTGCATTA-3'	This paper	N/A
sgRNA targeting mCherry 5'-CTCCGAGCGGATGTACCCCG-3'	This paper	N/A
Recombinant DNA		
envelope plasmid pMD2.G	Addgene	Cat# 12259; RRID:Addgene_12259
packing plasmid psPAX2	Addgene	Cat# 12260; Addgene_12260
lentiCRISPRv2	Addgene	Cat# 52961; Addgene_52961
pGL3/NF-κB-luc	Zhijie Chang's Lab	http://www.jbc.org/content/290/2/861.long
pRL-TK	Zhijie Chang's Lab	http://www.jbc.org/content/290/2/861.long
IL-1RI-FL-pcdna3.1-myc-his	This paper	N/A
IL-1RAcP-FL-pcdna3.1-HA-his	This paper	N/A
ST2-FL-pcdna3.1-myc-his	This paper	N/A
IL-1Rrp2-FL-pcdna3.1-myc-his	This paper	N/A
IL-18Rα-FL-pcdna3.1-myc-his	This paper	N/A
IL-18Rβ-FL-pcdna3.1-HA-his	This paper	N/A
IL-18Rβ-FL-pcdna3.1-flag	This paper	N/A
IL-1RAcP-FL-RI-pcdna3.1-HA-his	This paper	N/A
IL-1RAcP-FL-RII-pcdna3.1-HA-his	This paper	N/A
IL-1RAcP-FL-ST2-pcdna3.1-HA-his	This paper	N/A
IL-18Rβ-FL-18Rα-pcdna3.1-flag	This paper	N/A
Software and Algorithms		
SCÅTTER	Developed by Robert Rambo at the Diamond Light Source (Didcot, UK)	http://www.bioisis.net/tutorial/9
GNOM	Svergun, 1992	https://www.embl-hamburg.de/biosaxs/gnom.html
MODELLER	Sali and Blundell, 1993	https://salilab.org/modeller/
BILBOMD	Pelikan et al., 2009	http://bl1231.als.lbl.gov/bilbomd
FoXS	Schneidman-Duhovny et al., 2013	https://modbase.compbio.ucsf.edu/foxs/
Multi-FoXS	Schneidman-Duhovny et al., 2016	https://modbase.compbio.ucsf.edu/multifoxs/
CHIMERA	Pettersen et al., 2004	https://www.cgl.ucsf.edu/chimera/
CHARMM-GUI	Jo et al., 2008	http://www.charmm-gui.org/